

## A ROBUST NUMERICAL SCHEME FOR SINGULARLY PERTURBED DELAY PARABOLIC INITIAL-BOUNDARY-VALUE PROBLEMS ON EQUIDISTRIBUTED GRIDS\*

S. GOWRISANKAR<sup>†</sup> AND SRINIVASAN NATESAN<sup>‡</sup>

*This paper is dedicated to Professor Carlos Conca on the occasion of his 60th birthday.*

**Abstract.** In this article, we propose a parameter-uniform computational technique to solve singularly perturbed delay parabolic initial-boundary-value problems exhibiting parabolic boundary layers. The domain is discretized by a uniform mesh in the time direction and a nonuniform mesh for the spatial variable obtained via the equidistribution of a monitor function. The numerical scheme consists of the implicit Euler scheme for the time derivative and the classical central difference scheme for the spatial derivative. A truncation error analysis and a stability analysis are carried out. It is shown that the method converges uniformly in the discrete supremum norm with an optimal error bound. Error estimates are derived, and numerical examples are presented.

**Key words.** singularly perturbed delay parabolic problem, boundary layers, uniform convergence, equidistribution grid, monitor function

**AMS subject classifications.** 65M06, 65M12

**1. Introduction.** Let  $\Omega = (0, 1)$ ,  $D = \Omega \times (0, T]$ , and  $\Gamma = \Gamma_l \cup \Gamma_b \cup \Gamma_r$ , where  $\Gamma_l$  and  $\Gamma_r$  are the left- and right-hand sides of the rectangle  $D$  corresponding to  $x = 0$  and  $x = 1$ , respectively, and  $\Gamma_b = \overline{\Omega} \times [-\tau, 0]$ , where  $\overline{\Omega} = [0, 1]$ . In this paper, we devise an  $\varepsilon$ -uniform numerical method for the following class of singularly perturbed delay parabolic initial-boundary-value problems:

$$(1.1) \quad \begin{aligned} \left( \frac{\partial}{\partial t} + \mathcal{L}_\varepsilon \right) u(x, t) &= -b(x, t)u(x, t - \tau) + f(x, t), & (x, t) \in D, \\ u(x, t) &= \phi_b(x, t), & (x, t) \in \Gamma_b, \\ u(0, t) &= \phi_l(t), & \text{on } \Gamma_l = \{(0, t) : 0 \leq t \leq T\}, \\ u(1, t) &= \phi_r(t), & \text{on } \Gamma_r = \{(1, t) : 0 \leq t \leq T\}, \end{aligned}$$

where

$$\mathcal{L}_\varepsilon u(x, t) = -\varepsilon u_{xx}(x, t) + a(x)u(x, t),$$

$0 < \varepsilon \leq 1$  and  $\tau > 0$  are given constants,  $a(x), b(x, t), f(x, t), (x, t) \in \overline{D}$ , and  $\phi_l(t), \phi_r(t), \phi_b(x, t), (x, t) \in \Gamma$ , are sufficiently smooth and bounded functions, where

$$a(x) \geq 0, \quad b(x, t) \geq \beta > 0, \quad (x, t) \in \overline{D}.$$

The terminal time  $T$  is assumed to satisfy the condition  $T = k\tau$  for some positive integer  $k$ . The required compatibility conditions at the corner points and for the delay terms are

$$\phi_b(0, 0) = \phi_l(0), \quad \phi_b(1, 0) = \phi_r(0),$$

\*Received April 4, 2014. Accepted July 30, 2014. Published online on November 13, 2014. Recommended by K. Burrage.

<sup>†</sup>Department of Mathematics, National Institute of Technology Patna, Patna-800 005, India. (s.gowri@nitp.ac.in).

<sup>‡</sup>Indian Institute of Technology Guwahati, Guwahati-781 039, India. (natesan@iitg.ernet.in).

and

$$(1.2) \quad \begin{aligned} \frac{d\phi_l(0)}{dt} - \varepsilon \frac{\partial^2 \phi_b(0,0)}{\partial x^2} + a(0)\phi_b(0,0) &= -b(0,0)\phi_b(0,-\tau) + f(0,0), \\ \frac{d\phi_r(0)}{dt} - \varepsilon \frac{\partial^2 \phi_b(1,0)}{\partial x^2} + a(1)\phi_b(1,0) &= -b(1,0)\phi_b(1,-\tau) + f(1,0). \end{aligned}$$

Note that  $\phi_l(t)$ ,  $\phi_b(x, t)$ , and  $\phi_r(t)$  are assumed to be smooth for (1.2) to make sense. Under the above assumptions and conditions, problem (1.1) has a unique solution [1].

A numerical treatment of the IBVP (1.1) is difficult because of the presence of boundary layers in its solution. In particular, the classical finite difference methods fail to yield satisfactory numerical results on uniform meshes, and to obtain stability, one has to reduce the spatial step-size in relation to  $\varepsilon$ . The same is true for finite element methods in the case of a uniform mesh and polynomial basis functions. Basically, by these methods one cannot obtain  $\varepsilon$ -uniform error estimates. When regular boundary layers are present, it is possible to construct an  $\varepsilon$ -uniform method by using appropriately fitted finite difference operators (i.e., finite difference schemes with fitting factors) on uniform meshes. However, in [16] it is proved that this approach is not possible when parabolic boundary layers are present; more details can be found in [11]. One can refer to the books of Farrell et al. [5] and Roos et al. [15] for further results related to the theory and numerics of singularly perturbed parabolic problems. We also refer to the articles [13, 14] for efficient numerical methods for singular perturbation problems arising in chemical reactor theory using asymptotic approximations by applying various methods.

There are several numerical methods in the literature for singularly perturbed delay parabolic PDEs. Often piecewise-uniform Shishkin-type meshes are used for parameter-uniform convergence. Piecewise-uniform meshes are generated by using information about the layer locations and width, and this yields a second-order approximation in space up to a logarithmic factor. To overcome such difficulties and improve the convergence rate, adaptive meshes are used and are generated by equidistributing positive monitor functions. Different type of monitor functions are employed for singularly perturbed ordinary differential equations. In [9], the arc-length monitor function is used for quasi-linear one-dimensional convection-diffusion problems, while in [2, 3], the singular part of the solution is used for ordinary differential equations of reaction-diffusion and convection-diffusion type, respectively.

The main goal of this paper is to provide an  $\varepsilon$ -uniform numerical method for the IBVP (1.1) with an adaptive mesh. We obtain the adaptive mesh through the idea of an equidistribution of the singular component of  $u(x, t)$  at some fixed time  $T_0$ ,  $0 < T_0 \leq T$ , because the problem (1.1) exhibits boundary layers along boundaries that do not depend on time. One can also refer to [2, 3, 6, 7, 9, 12] for the stationary problem where an adaptive mesh is applied. In this method, the time derivative is replaced by the backward difference scheme, and the spatial derivative is replaced by the central difference scheme. The proposed scheme is parameter-uniform convergent of order  $O(\Delta t + N^{-2})$ , which is optimal compared to other methods in the literature [1, 10]. It is shown that the method converges uniformly in the discrete supremum norm with an optimal error bound. In this paper, truncation errors are estimated, a stability analysis is carried out, and  $\varepsilon$ -uniform error estimates are obtained. We show that the numerical solution converges uniformly of second order in the space variable as it is also indicated by the tables and figures in Section 5.

The rest of the paper is organized as follows: in Section 2, we provide a-priori bounds for the derivatives of the analytical solution via a decomposition. Section 3 introduces the implicit upwind finite difference scheme and also an adaptive spatial grid via the equidistribution

principle. Moreover, we present the detailed numerical algorithm in Section 3.3. Afterwards, we carry out the error analysis for the upwind scheme in Section 4 and prove the main theoretical result, i.e., the  $\varepsilon$ -uniform optimal error bounds of the implicit upwind scheme for the adaptive mesh. In Section 5, we present numerical results for linear test problems to validate the theoretical results. Finally in Section 6, we summarize the main conclusions.

Throughout this paper,  $C$  denotes a generic positive constant independent of  $\varepsilon$ ,  $N$ ,  $M$ , and the meshes  $(x_i, t_n)$ , where  $N$  and  $M$  are the number of mesh-intervals in the spatial and temporal directions, respectively. The norm  $\|\cdot\|_D$  denotes the supremum norm on the domain  $D$ . In the analysis, we assume that  $\sqrt{\varepsilon} \leq N^{-1}$ , which is the case of actual interest from the practical point of view. It can also be replaced by the hypothesis that  $\sqrt{\varepsilon} \leq CN^{-1}$  for some fixed constant  $C$  without altering the conclusions of this paper.

**2. Analytic solution.** In this section we present some bounds for the analytical solution  $u(x, t)$  of (1.1) and its partial derivatives and the maximum principle for the differential operator.

The reduced problem, by setting the parameter value  $\varepsilon = 0$  and removing the boundary conditions in (1.1), is

$$(2.1) \quad \begin{aligned} (u_0)_t(x, t) - a(x)u_0(x, t) &= -b(x, t)u_0(x, t - \tau) + f(x, t), & (x, t) \in D, \\ u_0(x, t) &= \phi_b(x, t), & (x, t) \in \Gamma_b. \end{aligned}$$

It is clear that the solution of (1.1) forms boundary layers on  $\Gamma_l$  and  $\Gamma_r$  in order to satisfy the boundary conditions. The characteristics of (2.1) are the vertical lines  $x = C$ , which implies that any boundary layer arising in the solution is of parabolic type. This type of problem can be solved by fixing the spatial grid for all temporal levels.

The differential operator in (1.1) satisfies the following maximum principle. Here  $\phi$  on  $\Gamma$  is defined by

$$\phi = \phi_l \text{ on } \Gamma_l, \quad \phi = \phi_r \text{ on } \Gamma_r, \quad \phi = \phi_b \text{ on } \Gamma_b.$$

**MAXIMUM PRINCIPLE.** Let  $\Psi(x, t)$  be a sufficiently smooth function satisfying  $\Psi(x, t) \geq 0$  on  $\Gamma$ . Then  $(\frac{\partial}{\partial t} + \mathcal{L}_\varepsilon) \Psi(x, t) \geq 0$  in  $D$  implies that  $\Psi(x, t) \geq 0$  in  $\bar{D}$ .

The following theorem gives stability of the continuous operator  $(\frac{\partial}{\partial t} + \mathcal{L}_\varepsilon)$  and an  $\varepsilon$ -uniform bound for the problem (1.1) in the maximum norm.

**THEOREM 2.1.** *Let  $v$  be any function in the domain of definition of the differential operator  $(\frac{\partial}{\partial t} + \mathcal{L}_\varepsilon)$  in (1.1). Then*

$$\|v\| \leq (1 + \alpha T) \max \left\{ \left\| \left( \frac{\partial}{\partial t} + \mathcal{L}_\varepsilon \right) v \right\|, \|v\|_\Gamma \right\},$$

and any solution of  $u$  of (1.1) has the  $\varepsilon$ -uniform upper bound

$$\|u\| \leq (1 + \alpha T) \max \{ \|f\|, \|\phi\|_\Gamma \},$$

where the constant  $\alpha = \max_{\bar{\Omega}} \{0, 1 - a\} \leq 1$ .

**THEOREM 2.2.** *Let the data  $a \in C^{2+\alpha}(\bar{\Omega})$ ,  $b, f \in C^{(2+\alpha, 1+\alpha/2)}(\bar{D})$ ,  $\phi_l \in C^{2+\alpha/2}([0, T])$ ,  $\phi_b \in C^{(4+\alpha, 2+\alpha/2)}(\Gamma_b)$ ,  $\phi_r \in C^{2+\alpha/2}([0, T])$ ,  $\alpha \in (0, 1)$  with compatibility conditions of sufficiently high order at the corners fulfilled. Then (1.1) has a unique solution  $u$  and  $u \in C^{(4+\alpha, 2+\alpha/2)}(\bar{D})$ . Furthermore, the derivatives of the solution  $u$  satisfy, for all non-negative integers  $i, j$  such that  $0 \leq i + 2j \leq 4$ ,*

$$\left\| \frac{\partial^{i+j} u}{\partial x^i \partial t^j} \right\|_{\bar{D}} \leq C\varepsilon^{-i/2}.$$

*Proof.* The proof of this theorem can be found in [1].  $\square$

The above bounds do not contain an explicit dependence on the boundary layer. Therefore, to obtain stronger estimates of the solution  $u(x, t)$  and its partial derivatives, we decompose  $u(x, t)$  into its smooth and singular components.

Let  $u$  be the solution of (1.1) and write

$$u = v + w,$$

where  $v$  and  $w$  are the smooth and singular components of  $u$  defined in the following way. The smooth component is further decomposed into

$$v = v_0 + \varepsilon v_1,$$

where  $v_0, v_1$  are defined by

$$\begin{aligned} (v_0)_t + av_0 &= -bv_0(x, t - \tau) + f, & (x, t) \in D, \\ v_0(x, t) &= \phi_b(x, t), & (x, t) \in \Gamma_b, \end{aligned}$$

and

$$\begin{aligned} \left( \frac{\partial}{\partial t} + \mathcal{L}_\varepsilon \right) v_1 &= -bv_1(x, t - \tau) + (v_0)_{xx}, & (x, t) \in D, \\ v_1(x, t) &= 0, & (x, t) \in \Gamma. \end{aligned}$$

By definition of  $v_0$  and  $v_1$ , the smooth component  $v$  and the singular component  $w$  can be defined as follows:

$$\begin{aligned} \left( \frac{\partial}{\partial t} + \mathcal{L}_\varepsilon \right) v(x, t) &= -bv(x, t - \tau) + f, & (x, t) \in D, \\ v(x, t) &= \phi_b(x, t), & (x, t) \in \Gamma_b, \\ v(0, t) &= v_0(0, t), & (x, t) \in \Gamma_l, \\ v(1, t) &= v_0(1, t), & (x, t) \in \Gamma_r, \end{aligned}$$

and

$$\begin{aligned} \left( \frac{\partial}{\partial t} + \mathcal{L}_\varepsilon \right) w(x, t) &= -bw(x, t - \tau), & (x, t) \in D, \\ w(x, t) &= 0, & (x, t) \in \Gamma_b, \\ w(0, t) &= \phi_l(t) - v_0(0, t), & (x, t) \in \Gamma_l, \\ w(1, t) &= \phi_r(t) - v_0(1, t), & (x, t) \in \Gamma_r. \end{aligned}$$

We further decompose the singular component into a left and right layer component,  $w_l$  and  $w_r$ , respectively, as follows:

$$(2.2) \quad w(x, t) = w_l(x, t) + w_r(x, t),$$

where  $w_l$  and  $w_r$  satisfy

$$\begin{aligned} \left( \frac{\partial}{\partial t} + \mathcal{L}_\varepsilon \right) w_l(x, t) &= -bw_l(x, t - \tau), & (x, t) \in D, \\ w_l(0, t) &= \phi_l(t) - v_0(0, t), & (x, t) \in \Gamma_l, \\ w_l(x, t) &= 0, & (x, t) \in \Gamma_b \cup \Gamma_r, \end{aligned}$$

and

$$\begin{aligned}
 \left(\frac{\partial}{\partial t} + \mathcal{L}_\varepsilon\right) w_r(x, t) &= -b w_r(x, t - \tau), & (x, t) \in D, \\
 w_r(1, t) &= \phi_r(t) - v_0(1, t), & (x, t) \in \Gamma_r, \\
 w_r(x, t) &= 0, & (x, t) \in \Gamma_b \cup \Gamma_l.
 \end{aligned}$$

The following theorem provides the bounds for the smooth component  $v$ , the singular component  $w$ , and their partial derivatives, which play a crucial role in the error analysis in Section 4.

**THEOREM 2.3.** *Assume that  $a \in \mathcal{C}^{4+\alpha}(\overline{\Omega})$ ,  $b, f \in \mathcal{C}^{(4+\alpha, 2+\alpha/2)}(\overline{D})$ ,  $\phi_l \in \mathcal{C}^{3+\alpha/2}([0, T])$ ,  $\phi_b \in \mathcal{C}^{(6+\alpha, 3+\alpha/2)}(\Gamma_b)$ ,  $\phi_r \in \mathcal{C}^{3+\alpha/2}([0, T])$ ,  $\alpha \in (0, 1)$  with compatibility conditions of sufficiently high order at the corners fulfilled. Then, for integers  $i, j$  such that  $0 \leq i + 2j \leq 4$ , we have the estimates*

$$\begin{aligned}
 (2.3) \quad \left\| \frac{\partial^{i+j} v}{\partial x^i \partial t^j} \right\|_{\overline{D}} &\leq C(1 + \varepsilon^{1-i/2}), \\
 \left| \frac{\partial^{i+j} w_l}{\partial x^i \partial t^j}(x, t) \right| &\leq C\varepsilon^{-i/2} e^{-x/\sqrt{\varepsilon}}, & (x, t) \in \overline{D}, \\
 \left| \frac{\partial^{i+j} w_r}{\partial x^i \partial t^j}(x, t) \right| &\leq C\varepsilon^{-i/2} e^{-(1-x)/\sqrt{\varepsilon}}, & (x, t) \in \overline{D},
 \end{aligned}$$

where  $C$  is independent of  $\varepsilon$ .

*Proof.* The proof of this theorem can be found in [1]. □

**THEOREM 2.4.** *The partial derivatives of  $w(x, t)$  satisfy*

$$\left| \frac{\partial^{i+j} w}{\partial x^i \partial t^j} \right| \leq C\varepsilon^{-i/2} \{e^{-x/\sqrt{\varepsilon}} + e^{-(1-x)/\sqrt{\varepsilon}}\}, \quad (x, t) \in \overline{D},$$

for integers  $i, j$  such that  $0 \leq i + 2j \leq 4$ .

*Proof.* The proof of the theorem is completed by using the estimates of Theorem 2.3 and the decomposition (2.2). □

**3. Numerical solution.** In this section, we discretize the parabolic delay IBVP (1.1). The time derivative is replaced by the backward difference scheme, and the spatial derivative is replaced by the central difference scheme. Subsequently, we introduce the equidistribution grid and derive a finite difference scheme. Finally, we provide the numerical algorithm for obtaining the equidistributed grids.

**3.1. Finite difference scheme.** On the time domain  $[0, T]$ , we introduce equidistant meshes with a uniform time step  $\Delta t$  such that

$$\Lambda_t^M = \{t_n = n\Delta t, n = 0, \dots, M, \Delta t = T/M\},$$

where  $M$  denotes the number of mesh elements in the  $t$ -direction on the interval  $[0, T]$ , and the step length  $\Delta t$  satisfies the constraint  $p\Delta t = \tau$ , where  $p$  is a positive integer,  $t_n = n\Delta t$ ,  $n \geq -p$ . We consider the finite difference approximation of (1.1) on a non-uniform spatial discretization

$$\Omega_x^N = \{0 = x_0 < x_1 < \dots < x_N = 1\},$$

and denote the spatial step sizes by

$$h_i = x_i - x_{i-1}, \quad i = 1, \dots, N.$$

We use the methods of steps to prove  $\varepsilon$ -uniform convergence in Section 4. Now we describe the discretization of the domains in a systematic way. We define discretized domains  $D^N = \Omega_x^N \times \Lambda_t^M$ ,  $\Gamma_b^N = \Omega_x^N \times \Lambda_t^p$ , where  $\Lambda_t^p$  represents  $p$  uniform mesh elements in  $[-\tau, 0]$ . The boundary points  $\Gamma^N$  of  $D^N$  are  $\Gamma^N = D^N \cap \Gamma$ . Similarly, we define the left and right boundary points by  $\Gamma_l^N = D^N \cap \Gamma_l$  and  $\Gamma_r^N = D^N \cap \Gamma_r$ , respectively.

We further introduce  $D_j^N = \Omega_x^N \times \Lambda_{j,t}^p$ , where  $\Lambda_{j,t}^p$  represents  $p$  uniform mesh elements in  $[(j-1)\tau, j\tau]$ , for  $j = 1, 2, \dots, k$ . From the above discretization we can also observe that  $D^N = \bigcup_{j=1}^k D_j^N$ . These notations are primarily used in Section 4, where the errors in the numerical solutions are analyzed with respect to  $\varepsilon$ -uniform convergence.

Before describing the scheme, for a given mesh function  $v(x_i, t_n) = v_i^n$ , define the forward and backward differences  $\delta_x^+$ ,  $\delta_x^-$  in space by

$$\delta_x^+ v_i^n = \frac{v_{i+1}^n - v_i^n}{h_{i+1}}, \quad \delta_x^- v_i^n = \frac{v_i^n - v_{i-1}^n}{h_i},$$

respectively, the second-order finite difference operator  $\delta_x^2$  as

$$\delta_x^2 v_i^n = \frac{2(\delta_x^+ v_i^n - \delta_x^- v_i^n)}{h_i + h_{i+1}},$$

and the backward difference operator  $\delta_t$  in time by

$$\delta_t v_i^n = \frac{v_i^n - v_i^{n-1}}{\Delta t}.$$

We discretize equation (1.1) by means of the backward Euler scheme for the time derivative and the central difference for the spatial derivative. Hence, the discretization of (1.1) takes the form

$$(3.1) \quad \begin{aligned} (\delta_t + L_\varepsilon) U_i^{n+1} &= -b(x_i, t_{n+1})U_i^{n-p+1} + f(x_i, t_{n+1}), \quad \text{for } i = 1, \dots, N-1, \\ U_0^{n+1} &= \phi_l(t_{n+1}), \\ U_N^{n+1} &= \phi_r(t_{n+1}), \\ U_i^{-j} &= \phi_b(x_i, -t_j), \quad \text{for } i = 1, \dots, N-1, \end{aligned}$$

where  $L_\varepsilon U_i^{n+1} = -\varepsilon \delta_x^2 U_i^{n+1} + a_i U_i^{n+1}$ .

After rearranging the terms in (3.1), we obtain the following form of the difference scheme:

$$(3.2) \quad \begin{aligned} r_i^- U_{i-1}^{n+1} + r_i^c U_i^{n+1} + r_i^+ U_{i+1}^{n+1} &= g_i^n, \quad \text{for } i = 1, \dots, N-1, \\ U_0^{n+1} &= \phi_l(t_{n+1}), \\ U_N^{n+1} &= \phi_r(t_{n+1}), \\ U_i^{-j} &= \phi_b(x_i, -t_j), \quad \text{for } i = 1, \dots, N-1, \end{aligned}$$

where

$$\begin{aligned} r_i^- &= \frac{-2\varepsilon \Delta t}{h_i(h_i + h_{i+1})}, & r_i^+ &= \frac{-2\varepsilon \Delta t}{h_{i+1}(h_i + h_{i+1})}, & r_i^c &= 1 + \Delta t a_i - r_i^- - r_i^+, \\ a_i &= a(x_i), & g_i^n &= U_i^n + \Delta t \left\{ -b(x_i, t_{n+1})U_i^{n-p+1} + f(x_i, t_{n+1}) \right\}. \end{aligned}$$

To determine the value of the monitor function (3.6), we have to know the approximate value of the singular component  $w(x, t)$ . To calculate the numerical value  $W_i^n$  of  $w(x_i, t_n)$ , we use the numerical approximate value  $V_i^n$  of  $v(x_i, t_n)$  from the following recurrence relation:

$$(3.3) \quad \begin{aligned} (1 + \Delta t a(x_i))V_i^{n+1} &= V_i^n + \Delta t \left\{ -b(x_i, t_{n+1})V_i^{n-p+1} + f(x_i, t_{n+1}) \right\}, \\ V_i^{-j} &= \phi_b(x_i, -t_j), \quad \text{for } i = 1, \dots, N. \end{aligned}$$

**3.2. Adaptive spatial grids via equidistribution.** Since the solution  $u(x, t)$  of the IBVP (1.1) exhibits boundary layers, one has to use layer-adapted nonuniform spatial grids, which are fine inside the boundary layer region and coarse in the outer region. To obtain such a grid, we use the idea of equidistribution of a positive monitor function given in (3.6). Here we consider the equidistribution of  $u(x, t)$  at some fixed time  $T_0$ ,  $0 < T_0 \leq T$ , because the problem (1.1) exhibits regular layers along the boundaries, which do not have any impact on the temporal component. Moreover, we assume that  $u(x, T_0)$  exhibits layer phenomena.

A grid is said to be equidistributing  $u(x, T_0)$  if

$$(3.4) \quad \int_{x_{i-1}}^{x_i} M(u(s, T_0), s) ds = \int_{x_i}^{x_{i+1}} M(u(s, T_0), s) ds, \quad i = 1, \dots, N-1,$$

where  $M(u(x, T_0), x)$  is a strictly positive,  $\mathcal{L}_1$ -integrable function. Equation (3.4) can also be written in the form

$$(3.5) \quad \int_{x_{i-1}}^{x_i} M(u(s, T_0), s) ds = \frac{1}{N} \int_0^1 M(u(s, T_0), s) ds, \quad i = 1, \dots, N.$$

Here, we consider the monitor function

$$(3.6) \quad M(u(x, T_0), x) = \alpha_c + |w_{xx}(x, T_0)|^{1/m}, \quad m \geq 2,$$

where  $\alpha_c$  is a positive constant that is independent of  $N$  and  $w(x, t)$  is the singular component of  $u(x, t)$ . The one-dimensional version of the monitor function (3.6) given by Beckett and Mackenzie [2] suggests that in order to distribute the grid points evenly, we take

$$(3.7) \quad \alpha_c = \int_0^1 |w_{xx}(s, T_0)|^{1/m} ds.$$

This choice of  $\alpha_c$  helps to distribute the number of mesh points inside and outside the boundary layer region equally. The effect of increasing  $m$  is to smooth out the monitor function, which in turn leads to a smoother distribution of the grid points. In [2], the influence of the parameter  $m$  can clearly be observed. In all of our numerical experiments we take  $m = 2$ .

In order to compute the value of the monitor function at the  $i$ th interior node of the spatial mesh,  $M_i$ , we assume that  $w(x_i, T_0) = W_i^S$ , where  $S\Delta t = T_0$ , and define

$$(3.8) \quad M_i = \alpha_{dis} + |\delta_x^2 W_i^S|^{1/m}, \quad \text{for } i = 1, \dots, N-1,$$

where  $\alpha_{dis}$  is the discrete form of (3.7), which can be written as

$$\alpha_{dis} = h_1 |\delta_x^2 W_1^S|^{1/m} + \sum_{i=2}^{N-1} h_i \left\{ \frac{|\delta_x^2 W_{i-1}^S|^{1/m} + |\delta_x^2 W_i^S|^{1/m}}{2} \right\} + h_N |\delta_x^2 W_{N-1}^S|^{1/m}.$$

For a truly adaptive algorithm, the monitor function has to be approximated using the numerical solution. For example, a simple discretization of (3.4) results in the set of equations

$$M_{i-1/2}(x_i - x_{i-1}) = M_{i+1/2}(x_{i+1} - x_i), \quad \text{for } i = 1, \dots, N-1,$$

where  $M_{i+1/2}$  is an approximation to  $M(u(x_{i+1/2}, T_0), x_{i+1/2})$ . This is equivalent to an approximation of the monitor function by a piecewise constant function. The detailed numerical algorithm for obtaining the equidistribution grids is given in Section 3.3.

LEMMA 3.1. *For  $i = 1, 2, \dots, N$ , the grid spacing satisfies*

$$h_i \leq CN^{-1}.$$

*Proof.* From the equidistribution principle (3.5), we have

$$\int_{x_{i-1}}^{x_i} M(u(s, T_0), s) ds = \frac{1}{N} \int_0^1 M(u(s, T_0), s) ds, \quad i = 1, \dots, N.$$

Applying the Mean Value Theorem, we get

$$h_i M(u(\eta_i, T_0), \eta_i) = N^{-1} \int_0^1 M(u(s, T_0), s) ds$$

for some  $\eta_i \in (x_{i-1}, x_i)$ . And therefore, we have

$$h_i = N^{-1} \frac{\int_0^1 M(u(s, T_0), s) ds}{M(u(\eta_i, T_0), \eta_i)} \leq CN^{-1},$$

which is the desired result.  $\square$

**3.3. The numerical algorithm.** To get the equidistribution grid and the corresponding numerical solution, we use the following algorithm:

1. Set  $k = 0$ . Take the uniform spatial mesh  $\{x_i^{(0)}\}$  as initial value for the iteration. Choose a constant  $C > 1$  that controls when the algorithm has to be terminated.
2. Compute the discrete solution  $\{U_i^{n,(k)}\}$  and  $\{V_i^{n,(k)}\}$  satisfying (3.2) and (3.3), respectively, with the help of the spatial mesh  $\{x_i^{(k)}\}$ .
3. Find the singular component of the discrete solution by  $W_i^{n,(k)} = U_i^{n,(k)} - V_i^{n,(k)}$ .
4. For a given mesh  $\{x_i^{(k)}\}$  and the singular component of the discrete solution  $\{W_i^{n,(k)}\}$ , set

$$H_i^{(k)} = \left( \frac{M_{i-1}^{(k)} + M_i^{(k)}}{2} \right) (x_i^{(k)} - x_{i-1}^{(k)}), \quad \text{for } i = 1, \dots, N,$$

where  $M_i^{(k)}$  is calculated from (3.8), and set  $M_0^{(k)} = M_1^{(k)}$  and  $M_N^{(k)} = M_{N-1}^{(k)}$ .

5. Set  $L_0 = 0$  and  $L_i = \sum_{j=1}^i H_j^{(k)}$ , for  $i = 1, \dots, N$ . Define

$$C^{(k)} := \frac{N}{L_N} \max_{i=0,1,\dots,N} H_i^{(k)}.$$

6. If  $C^{(k)} \leq C$ , then go to Step 9.
7. Set  $Y_i = iL_N/N$ , for  $i = 0, 1, \dots, N$ . Interpolate the points  $(L_i, x_i)$ . Generate the new mesh  $\{x_i^{(k+1)}\}$  by evaluating this interpolant at  $Y_i$ , for  $i = 0, 1, \dots, N$ .



8. Set  $k = k + 1$ . Return to Step 2.

9. Take  $\{x_i^{(k)}\}$  as the final mesh, and compute  $U_i^{n,(k)}$ ; then stop.

For convergence of this algorithm for stationary problems, one can refer to [9], where the authors analyzed a predetermined number of iterations with respect to  $\varepsilon$ -uniform convergence. The results are proved for the well-known *arc-length monitor function*, which is different from that one given in (3.6). More information can be found in [2, 3].

**4. Error analysis.** In this section, we carry out a stability analysis for the discrete operator defined in (3.1). Finally, we obtain an  $\varepsilon$ -uniform error estimate in the discrete maximum norm. The following lemma provides a stability result for a general numerical scheme for the IBVP (1.1). The proof of this lemma can be found in [15]. Here, we are only stating the result. Before that, we provide the definition of an  $M$ -matrix.

**DEFINITION 4.1** ( $M$ -matrix). *A matrix  $A$  is said to be an  $M$ -matrix if its entries  $a_{ij}$  satisfy  $a_{ij} \leq 0$  for  $i \neq j$  and its inverse  $A^{-1}$  exists with  $A^{-1} \geq 0$ .*

**LEMMA 4.2.** *Consider the IBVP (1.1) and the difference scheme (3.1). This difference scheme (excluding the initial and boundary conditions) can be written as*

$$(4.1) \quad \delta_t U^{n+1} + L_\varepsilon U^{n+1} := AU^{n+1} - DU^n = F^n, \quad \text{for } n = 0, \dots, M-1,$$

where  $U^n = (U_1^n, \dots, U_{N-1}^n)^T$ ,  $F^n$  is a vector independent of the computed solution, and  $A$  and  $D$  are matrices. Moreover,  $A$  is an  $M$ -matrix, and  $D \geq 0$ .

Let  $y$  and  $z$  be two mesh functions with  $y^n = (y_0^n, \dots, y_N^n)^T$  and  $z^n = (z_0^n, \dots, z_N^n)^T$ , for each  $n$ . Assume that  $|\delta_t y^{n+1} + L_\varepsilon y^{n+1}| \leq \delta_t z^{n+1} + L_\varepsilon z^{n+1}$ , for  $n = 0, \dots, M-1$ , and  $|y| \leq z$  on the boundary  $\Gamma_b \cup \Gamma_l \cup \Gamma_r$ . Then  $|y| \leq z$  on  $\bar{\Omega}_x^N \times \bar{\Omega}_t^M$ .

*Proof.* The difference scheme (3.1) can be written in the form (4.1), for  $n=0, \dots, p-1$ , with  $A = (a_{ij})$  and  $D = (d_{ij})$  as

$$a_{i,i-1} = \frac{r_i^-}{\Delta t}, \quad a_{i,i} = \frac{r_i^c}{\Delta t}, \quad a_{i,i+1} = \frac{r_i^+}{\Delta t}, \quad d_{i,i} = \frac{1}{\Delta t}.$$

A short calculation shows that the matrix  $A$  is an  $M$ -matrix and the matrix  $D$  satisfies  $D \geq 0$ . Therefore, the difference scheme satisfies the hypotheses of [15, Lemma 3.2], and the result follows immediately. The above argument can also be extended to other time steps.  $\square$

The finite difference operator  $(\delta_t + L_\varepsilon)$  in (3.1) satisfies the following discrete maximum principle on  $D^N$ .

**DISCRETE MAXIMUM PRINCIPLE.** Assume that  $\Psi(x_i, t_n)$  satisfies  $\Psi(x_i, t_n) \geq 0$  on  $(x_i, t_n) \in \Gamma^N$ . Then  $(\delta_t + L_\varepsilon) \Psi(x_i, t_n) \geq 0$  on  $(x_i, t_n) \in D^N$  implies that  $\Psi(x_i, t_n) \geq 0$  at each point  $(x_i, t_n) \in D^N$ .

Next, we provide an important theorem for the  $\varepsilon$ -uniform convergence of the numerical solution in the discrete maximum norm.

**THEOREM 4.3.** *Let  $u$  and  $U$  be, respectively, the continuous and the numerical solutions of the IBVPs (1.1) and (3.2) satisfying compatibility conditions of sufficiently high order at the corners. Then, we have the following bound*

$$(4.2) \quad \max_{i,n} |(u - U)(x_i, t_n)| \leq C[\Delta t + N^{-2}], \quad \text{for all } (x_i, t_n) \in D^N,$$

where  $U(x_i, t_n) = U_i^n$ .

*Proof.* We prove the theorem by the following steps. We first prove the result on the interval  $[0, \tau]$ , i.e., the time discretization parameter  $n$  varies from 0 to  $p$ . Let  $\eta_i^n = u_i^n - U_i^n$

be the truncation error of the computed solution at each mesh point  $(x_i, t_n)$ . We write the scheme (3.1) as

$$\delta_t U_i^n + L_\varepsilon U_i^n = -b_{i,n} \phi_b(x_i, t_{n-p}) + f_i^n, \quad i = 1, \dots, N-1, \quad n = 1, \dots, p.$$

Therefore, the truncation error of the above scheme can be expressed in the following way as in [4, 10]

$$\delta_t \eta_i^n + L_\varepsilon \eta_i^n = \chi_{1,i}^n + \chi_{2,i}^n, \quad \text{for } (x_i, t_n) \in D_1^N,$$

where  $\chi_{1,i}^n$  and  $\chi_{2,i}^n$  are defined as

$$\chi_{1,i}^n := L_\varepsilon U_i^n - (\mathcal{L}_\varepsilon u)_i^n \quad \text{and} \quad \chi_{2,i}^n := \delta_t u_i^n - (u_t)_i^n.$$

With this splitting of the truncation error, we can decompose the error  $\eta$  as  $\eta = \phi + \psi$ . Here, the function  $\phi_i^n$  is, for each fixed  $n = 0, \dots, p$ , the solution of the discrete two-point boundary-value problem

$$(4.3) \quad \begin{aligned} L_\varepsilon \phi_i^n &= \chi_{1,i}^n, & \text{for } i = 1, \dots, N-1, \\ \phi_0^n &= \phi_N^n = 0, \end{aligned}$$

and  $\psi_i^n$  is the solution of the discrete parabolic problem

$$\begin{aligned} \delta_t \psi_i^n + L_\varepsilon \psi_i^n &= \chi_{2,i}^n - \delta_t \phi_i^n, & \text{for } i = 1, \dots, N-1, \\ \psi_0^n &= \psi_N^n = 0, & \text{for } n = 1, \dots, p, \\ \psi_i^0 &= -\phi_i^0, & \text{for } i = 0, \dots, N. \end{aligned}$$

Equation (4.3) is a sequence of two-point boundary-value problems that have been discretized using  $L_\varepsilon$  with  $\chi_{1,i}^n$  playing the role of the truncation error, and its solution can be bounded using techniques from [3]. The problem (1.1) exhibits parabolic boundary layers, and the same is true for (4.3). Therefore, the following error bound derived in [3] can be invoked for all time steps,

$$(4.4) \quad |\phi_i^n| \leq CN^{-2}, \quad \text{for all } i, n \leq p,$$

using the assumption that  $N^{-1} \gg \sqrt{\varepsilon}$  and the fact that our problem exhibits parabolic boundary layers.

All that remains is to bound the other error component  $\psi$ . By Lemma 4.2 and a discrete maximum principle, we get the following bounds for the error component  $\psi$ ,

$$|\psi_i^n| \leq C \left( \max_i |\phi_i^0| + \max_{i,n} |\chi_{2,i}^n - \delta_t \phi_i^n| \right), \quad \text{for } i, n \leq p.$$

Using the bounds of  $\chi_{2,i}^n$  and (4.4), we obtain

$$(4.5) \quad |\psi_i^n| \leq C \left[ N^{-2} + \Delta t + \max_{i,n} |\delta_t \phi_i^n| \right], \quad \text{for } i, n \leq p.$$

It remains to bound  $\delta_t \phi$  in (4.5). Using the assumption that  $a(x)$  is independent of  $t$ , the definition (4.3) implies that  $\delta_t \phi$  satisfies

$$(4.6) \quad \begin{aligned} L_\varepsilon (\delta_t \phi)_i^n &= \delta_t \chi_{1,i}^n, & \text{for } i = 1, \dots, N-1, \\ (\delta_t \phi)_0^n &= (\delta_t \phi)_N^n = 0. \end{aligned}$$

To analyze the sequence of two-point boundary value problems (4.6), observe that the right-hand side of the above equation can be written as

$$\begin{aligned} \delta_t \chi_{1,i}^n &= \frac{1}{\Delta t} \left( \chi_{1,i}^n - \chi_{1,i}^{n-1} \right) \\ &= \frac{1}{\Delta t} \left( (L_\varepsilon u_i^n - (\mathcal{L}_\varepsilon u)_i^n) - (L_\varepsilon u_i^{n-1} - (\mathcal{L}_\varepsilon u)_i^{n-1}) \right) \\ &= \frac{1}{\Delta t} \left( (L_\varepsilon u_i^n - L_\varepsilon u_i^{n-1}) - ((\mathcal{L}_\varepsilon u)_i^n - (\mathcal{L}_\varepsilon u)_i^{n-1}) \right). \end{aligned}$$

Let  $\hat{\mathcal{L}}_\varepsilon u = -\varepsilon u_{xx}$  and  $\hat{L}_\varepsilon u_i^n = -\varepsilon \delta_x^2 u_i^n$ . That is,  $\hat{L}_\varepsilon u$  is the discretization of the continuous operator  $\mathcal{L}_\varepsilon u$ . Then, one can write the above formula as

$$\delta_t \chi_{1,i}^n = \frac{1}{\Delta t} \int_{t_{n-1}}^{t_n} \left[ \hat{L}_\varepsilon \frac{\partial}{\partial t} u(x_i, t) - \hat{\mathcal{L}}_\varepsilon \frac{\partial}{\partial t} u(x_i, t) \right].$$

By using Peano’s kernel theorem as in [8] and following the argument given in [4], we obtains the same estimate for  $\delta_t \chi_{1,i}^n$  as the bounds for the corresponding truncation error arising in [3] for a standard two-point reaction-diffusion boundary-value problem. Now analyzing the problem in the same way as (4.3), we obtain the following bound for  $\delta_t \phi_i^n$ ,

$$(4.7) \quad |\delta_t \phi_i^n| \leq CN^{-2}, \quad \text{for all } i, n \leq p.$$

Combining (4.4), (4.5), and (4.7), we arrive at

$$\max_{i,n} |(u - U)(x_i, t_n)| \leq C[\Delta t + N^{-2}], \quad \text{for all } (x_i, t_n) \in D_1^N,$$

where  $U(x_i, t_n) = U_i^n$ .

For  $t \geq \tau$  it is not possible to follow the above argument because the delay term  $u(x, t)$  depends on  $u(x, t - \tau)$ , which is unknown for  $t \geq \tau$ . For this reason, we have to estimate the difference between the numerical solution  $U$  and the exact solution  $u$  itself over the interval  $[\tau, 2\tau]$ . The proof of this estimate follows an approach of [1] in which a fitted piecewise uniform mesh is used.

Consider the following singularly perturbed delay parabolic equation on the domain  $D_2 = (0, 1) \times (\tau, 2\tau)$ :

$$(4.8) \quad \begin{aligned} \left( \frac{\partial}{\partial t} + \mathcal{L}_\varepsilon \right) u(x, t) &= -b(x, t)u(x, t - \tau) + f(x, t), & (x, t) \in D_2, \\ u(x, \tau) &= u(x, t(p)), & x \in \Omega, \\ u(0, t) &= \phi_0(t), & t \in [\tau, 2\tau], \\ u(1, t) &= \phi_1(t), & t \in [\tau, 2\tau]. \end{aligned}$$

We discretize (4.8) by means of the backward Euler scheme for the time derivative and the central difference quotient for the space derivative. Hence, the discretization takes the form

$$(4.9) \quad \begin{aligned} (\delta_t + L_\varepsilon) U(x_i, t_n) &\equiv \delta_t U_i^n - \varepsilon \delta_x^2 U_i^n + a U_i^n \\ &= -b_{i,n} U_i^{n-p} + f(x_i, t_n), & (x_i, t_n) \in D_2^N, \\ U(x_i, t_n) &= U_1(x_i, t_n), & (x_i, t_n) \in D_1^N, \\ U(0, t_n) &= \phi_0(t_n), & t_n \in \Lambda_{2,t}^p, \\ U(1, t_n) &= \phi_1(t_n), & t_n \in \Lambda_{2,t}^p, \end{aligned}$$

where  $U_1$  is the numerical solution calculated on  $D_1^N$ . The solution  $u$  of (4.8) is decomposed into smooth and singular components  $u = y + z$ . The smooth component  $y$  is further decomposed into  $y = y_0 + \varepsilon y_1$ , where  $y_0$  and  $y_1$  solve the following problems:

$$\begin{aligned} \frac{\partial y_0}{\partial t}(x, t) + ay_0(x, t) &= -by_0(x, t - \tau) + f(x, t), & (x, t) \in D_2, \\ y_0(x, t) &= u(x, t), & (x, t) \in \Omega \times [0, \tau], \end{aligned}$$

and

$$\begin{aligned} \left( \frac{\partial}{\partial t} + \mathcal{L}_\varepsilon \right) y_1(x, t) &= -by_1(x, t - \tau) + \frac{\partial^2 y_0}{\partial x^2}(x, t), & (x, t) \in D_2, \\ y_1(x, t) &= 0, & (x, t) \in \Omega \times [0, \tau], \\ y_1(0, t) &= 0, & t \in [\tau, 2\tau], \\ y_1(1, t) &= 0, & t \in [\tau, 2\tau]. \end{aligned}$$

By the above definition of  $y_0$  and  $y_1$ , the smooth component  $y$  satisfies

$$\begin{aligned} \left( \frac{\partial}{\partial t} + \mathcal{L}_\varepsilon \right) y(x, t) &= -by(x, t - \tau) + f(x, t), & (x, t) \in D_2, \\ y(x, t) &= u(x, t), & (x, t) \in \Omega \times [0, \tau], \\ y(0, t) &= y_0(0, t), & t \in [\tau, 2\tau], \\ y(1, t) &= y_0(1, t), & t \in [\tau, 2\tau]. \end{aligned}$$

The singular component  $z$  satisfies

$$\begin{aligned} \left( \frac{\partial}{\partial t} + \mathcal{L}_\varepsilon \right) z(x, t) &= -bz(x, t - \tau), & (x, t) \in D_2, \\ z(x, t) &= 0, & (x, t) \in \Omega \times [0, \tau], \\ z(0, t) &= \phi_l(t) - y_0(0, t), & t \in [\tau, 2\tau], \\ z(1, t) &= \phi_r(t) - y_0(1, t), & t \in [\tau, 2\tau]. \end{aligned}$$

The singular component  $z$  can be further decomposed as  $z = z_l + z_r$ , where the left- and right-hand side layer terms  $z_l$  and  $z_r$  satisfy

$$\begin{aligned} \left( \frac{\partial}{\partial t} + \mathcal{L}_\varepsilon \right) z_l(x, t) &= -bz_l(x, t - \tau), & (x, t) \in D_2, \\ z_l(x, t) &= 0, & (x, t) \in \Omega \times [0, \tau], \\ z_l(0, t) &= \phi_l(t) - y_0(0, t), & [\tau, 2\tau], \\ z_l(1, t) &= 0, & t \in [\tau, 2\tau], \end{aligned}$$

and

$$\begin{aligned} \left( \frac{\partial}{\partial t} + \mathcal{L}_\varepsilon \right) z_r(x, t) &= -bz_r(x, t - \tau), & (x, t) \in D_2, \\ z_r(x, t) &= 0, & (x, t) \in \Omega \times [0, \tau], \\ z_r(0, t) &= 0, & t \in [\tau, 2\tau], \\ z_r(1, t) &= \phi_r(t) - y_0(1, t), & t \in [\tau, 2\tau]. \end{aligned}$$

The numerical solution  $U$  of (4.9) can be decomposed into smooth and singular components in an analogous manner to the decomposition of the solution  $u$  of (4.8). That is,

$$U = Y + Z,$$

where  $Y$  is the solution of the following problem:

$$\begin{aligned} (\delta_t + L_\varepsilon) Y(x_i, t_n) &= -b_{i,n} Y(x_i, t_{n-p}) + f, & (x_i, t_n) &\in D_2^N, \\ Y(x_i, t_n) &= U_1(x_i, t_n), & (x_i, t_n) &\in D_1^N, \\ Y(0, t_n) &= y_0(0, t_n), & t_n &\in \Lambda_{2,t}^p, \\ Y(1, t_n) &= y_0(1, t_n), & t_n &\in \Lambda_{2,t}^p. \end{aligned}$$

By this equation, the approximation of the singular component  $Z$  satisfies

$$\begin{aligned} (\delta_t + L_\varepsilon) Z(x_i, t_n) &= -b_{i,n} Z(x_i, t_{n-p}), & (x_i, t_n) &\in D_2^N, \\ Z(x_i, t_n) &= 0, & (x_i, t_n) &\in D_1^N, \\ Z(0, t_n) &= \phi_l(t_n) - y_0(0, t_n), & t_n &\in \Lambda_{2,t}^p, \\ Z(1, t_n) &= \phi_r(t_n) - y_0(1, t_n), & t_n &\in \Lambda_{2,t}^p. \end{aligned}$$

Therefore, the error at the node  $(x_i, t_n)$  can be written as

$$(U - u)(x_i, t_n) = (Y - y)(x_i, t_n) + (Z - z)(x_i, t_n).$$

Thus,

$$|(U - u)(x_i, t_n)| \leq |(Y - y)(x_i, t_n)| + |(Z - z)(x_i, t_n)|.$$

By this inequality, it is enough to bound the error of the singular and the regular components by an optimal bound. The truncation error of the smooth component can be written as

$$\begin{aligned} (\delta_t + L_\varepsilon)(Y - y) &= -b_{i,n} Y(x_i, t_{n-p}) + f - (\delta_t + L_\varepsilon)y \\ &= b_{i,n}(y(x_i, t_{n-p}) - Y(x_i, t_{n-p})) + \left( \left( \frac{\partial}{\partial t} + \mathcal{L}_\varepsilon \right) - (\delta_t + L_\varepsilon) \right) y \\ &= b_{i,n}(u(x_i, t_{n-p}) - U_1(x_i, t_{n-p})) + \left( \left( \frac{\partial}{\partial t} + \mathcal{L}_\varepsilon \right) - (\delta_t + L_\varepsilon) \right) y. \end{aligned}$$

Therefore, we have

$$\begin{aligned} (\delta_t + L_\varepsilon)(Y - y) &= -b_{i,n}(u(x_i, t_{n-p}) - U_1(x_i, t_{n-p})) - \varepsilon \left( \frac{\partial^2}{\partial x^2} - \delta_x^2 \right) y + \left( \frac{\partial}{\partial t} - \delta_t \right) y. \end{aligned}$$

Now taking the modulus and using (4.2) for the first part, this reduces to

$$|(\delta_t + L_\varepsilon)(Y - y)(x_i, t_n)| \leq C(N^{-2} + \Delta t) + \varepsilon \left| \left( \frac{\partial^2}{\partial x^2} - \delta_x^2 \right) y \right| + \left| \left( \frac{\partial}{\partial t} - \delta_t \right) y \right|.$$

Using a Taylor series expansion, it is easy to show that

$$|(\delta_t + L_\varepsilon)(Y - y)(x_i, t_n)| \leq C \left( N^{-2} + \Delta t + (h_{i+1} + h_i)^2 \varepsilon \left\| \frac{\partial^4 y}{\partial x^4} \right\| + \Delta t \left\| \frac{\partial^2 y}{\partial t^2} \right\| \right).$$

Applying Lemma 3.1 and the bounds for the derivatives in (2.3), we obtain

$$|(\delta_t + L_\varepsilon)(Y - y)(x_i, t_n)| \leq C(N^{-2} + \Delta t), \quad \text{for } (x_i, t_n) \in D_2^N.$$

Now using the fact that the discrete operator  $(\delta_t + L_\varepsilon)$  satisfies a discrete maximum principle and the inverse operator is uniformly bounded, the above inequality can be reduced to

$$(4.10) \quad |(Y - y)(x_i, t_n)| \leq C(N^{-2} + \Delta t), \quad \text{for } (x_i, t_n) \in D_2^N.$$

To estimate the singular component of the error, we discretize  $Z$  in the same way as its continuous counterpart  $z$  is discretized,  $Z = Z_l + Z_r$ , where  $Z_l$  and  $Z_r$  correspond to the left and right layers of the numerical solutions, respectively. They are defined by

$$\begin{aligned} (\delta_t + L_\varepsilon) Z_l &= -b_{i,n} Z_l(x_i, t_{n-p}), & (x_i, t_n) &\in D_2^N, \\ Z_l(x_i, t_n) &= 0, & (x_i, t_n) &\in D_2^N, \\ Z_l(0, t_n) &= \phi_l(t_n) - y_0(0, t_n), & t_n &\in \Lambda_{2,t}^p, \\ Z_l(1, t_n) &= 0, & t_n &\in \Lambda_{2,t}^p, \end{aligned}$$

and

$$\begin{aligned} (\delta_t + L_\varepsilon) Z_r &= -b_{i,n} Z_r(x_i, t_{n-p}), & (x_i, t_n) &\in D_2^N, \\ Z_r(x_i, t_n) &= 0, & (x_i, t_n) &\in D_2^N, \\ Z_r(0, t_n) &= 0, & t_n &\in \Lambda_{2,t}^p, \\ Z_r(1, t_n) &= \phi_r(t_n) - y_0(1, t_n), & t_n &\in \Lambda_{2,t}^p. \end{aligned}$$

The error can then be written in the form

$$(Z - z)(x_i, t_n) = (Z_l - z_l)(x_i, t_n) + (Z_r - z_r)(x_i, t_n), \quad (x_i, t_n) \in D_2^N,$$

and the errors  $Z_l - z_l$  and  $Z_r - z_r$  associated with the boundary layers of  $\Gamma_l$  and  $\Gamma_r$ , respectively, can be estimated separately. Consider the error  $Z_l - z_l$ ,

$$\begin{aligned} (\delta_t + L_\varepsilon)(Z_l - z_l) &= \left( \left( \frac{\partial}{\partial t} + \mathcal{L}_\varepsilon \right) - (\delta_t + L_\varepsilon) \right) z_l \\ &= -\varepsilon \left( \frac{\partial^2}{\partial x^2} - \delta_x^2 \right) z_l + \left( \frac{\partial}{\partial t} - \delta_t \right) z_l. \end{aligned}$$

Taking the modulus and using a Taylor series expansion in time, we obtain

$$\begin{aligned} |(\delta_t + L_\varepsilon)(Z_l - z_l)| &\leq C \left( N^{-2} + \Delta t + \varepsilon \left\| \left( \frac{\partial^2}{\partial x^2} - \delta_x^2 \right) z_l \right\| + \Delta t \left\| \frac{\partial^2 z_l}{\partial t^2} \right\| \right) \\ &\leq C \left( N^{-2} + \Delta t + \varepsilon \left\| \left( \frac{\partial^2}{\partial x^2} - \delta_x^2 \right) z_l \right\| \right). \end{aligned}$$

By fixing  $t$ , the lateral part of the above inequality can be regarded as in [3] as the truncation error of the two point reaction-diffusion boundary value problem corresponding to the left-hand side layer. By this observation, the truncation error in space can be analyzed in the same way as in [3, Lemma 8, 9] with the only difference that there it is given for both layers, whereas we only require the part of the left-hand side layer. Hence, we obtain

$$|(\delta_t + L_\varepsilon)(Z_l - z_l)(x_i, t_n)| \leq C(N^{-2} + \Delta t), \quad (x_i, t_n) \in D_2^N.$$

Now using the fact that the discrete operator  $(\delta_t + L_\varepsilon)$  satisfies a discrete maximum principle and the inverse operator is uniformly bounded, the above inequality can be reduced to

$$(4.11) \quad |(Z_l - z_l)(x_i, t_n)| \leq C(N^{-2} + \Delta t), \quad \text{for } (x_i, t_n) \in D_2^N.$$

A similar analysis shows that the error corresponding to the right-hand side part can also be bounded as

$$(4.12) \quad |(Z_r - z_r)(x_i, t_n)| \leq C(N^{-2} + \Delta t), \quad \text{for } (x_i, t_n) \in D_2^N.$$

Combining (4.10), (4.11), and (4.12) completes the proof for the second interval  $[\tau, 2\tau]$ . Similarly, we can prove the estimate for successive intervals in the temporal direction.  $\square$

**5. Numerical results.** In this section, we present the numerical results obtained by the fully discrete scheme (3.2) for two test problems on a rectangular mesh  $D_\varepsilon^{N,M} = \Omega_x^N \times \Lambda_t^M$ , where  $\Omega_x^N$  is the equidistributed grid obtained from the numerical algorithm. In all the numerical experiments, we fix  $m = 2$ , which is used to define the monitor function (3.6). Moreover, in all the tables the results are given first for a coarsest discretization with  $N = 32$  and a time step  $\Delta t = 0.1$ , and each following column corresponds to a refined discretization compared to the previous one, such that  $N$  is multiplied by two and  $\Delta t$  is divided by four. The reason for dividing  $\Delta t$  by four is to justify the spatial order of convergence properly.

EXAMPLE 5.1. Consider the following singularly perturbed delay parabolic initial-boundary-value problem:

$$(5.1) \quad \begin{aligned} u_t(x, t) - \varepsilon u_{xx}(x, t) &= -2e^{-1}u(x, t-1), & (x, t) &\in (0, 1) \times (0, 2], \\ u(x, t) &= e^{-(t+x/\sqrt{\varepsilon})}, & (x, t) &\in [0, 1] \times [-1, 0], \\ u(0, t) &= e^{-t}, & t &\in [0, 2], \\ u(1, t) &= e^{-(t+1/\sqrt{\varepsilon})}, & t &\in [0, 2]. \end{aligned}$$

The exact solution is  $u(x, t) = e^{-(t+x/\sqrt{\varepsilon})}$ . From the exact solution, it is clear that there is a parabolic boundary layer only in a neighborhood of  $\Gamma_l$ , and there is no boundary layer along  $\Gamma_r$ .

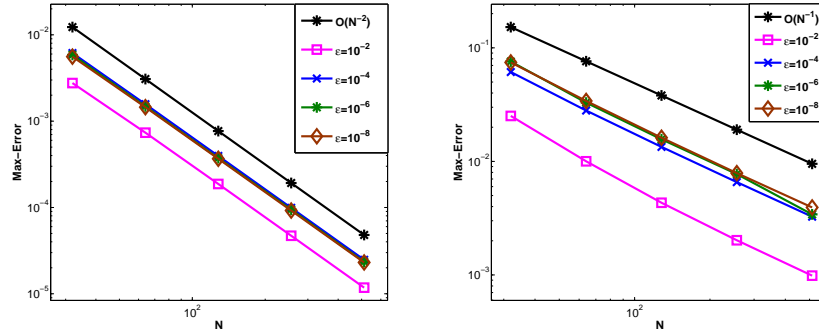
As the exact solution of the problem (5.1) is known, for each  $\varepsilon$ , we calculate the maximum pointwise error by

$$e_\varepsilon^{N,\Delta t} = \max_{(x_i, t_n) \in D_\varepsilon^{N,M}} |u(x_i, t_n) - U^{N,\Delta t}(x_i, t_n)|,$$

where  $u(x_i, t_n)$  and  $U^{N,\Delta t}(x_i, t_n)$ , respectively, denote the exact and the numerical solution obtained on the mesh with  $N$  mesh intervals in the spatial direction and  $M$  mesh intervals in the  $t$ -direction such that  $\Delta t = T/M$  is the uniform time step. In addition, we determine the corresponding order of convergence by

$$p_\varepsilon^{N,\Delta t} = \log_2 \left( \frac{e_\varepsilon^{N,\Delta t}}{e_\varepsilon^{2N,\Delta t/2}} \right).$$

The calculated maximum pointwise errors  $e_\varepsilon^{N,\Delta t}$  and the corresponding order of convergence  $p_\varepsilon^{N,\Delta t}$  for Example 5.1 are given in Table 5.1 and Table 5.2, respectively. From these results one can observe  $\varepsilon$ -uniform convergence of the numerical solution.



(a) Maximum pointwise error  $e_\varepsilon^{N, \Delta t}$  of the solution. (b) Maximum pointwise error  $r_\varepsilon^{N, \Delta t}$  of the normalized flux.

FIG. 5.1. Log-log plot for Example 5.1.

Furthermore, we calculate the normalized flux

$$F_\varepsilon u(x, t) = \sqrt{\varepsilon} \frac{\partial u(x, t)}{\partial x}$$

and its numerical approximation

$$F_\varepsilon^N U^{N, \Delta t}(x_i, t_n) = \sqrt{\varepsilon} \delta_x^+ U_i^n.$$

The errors in the normalized flux are calculated as

$$r_\varepsilon^{N, \Delta t} = \max_{1 \leq n \leq M} \|F_\varepsilon u(x_0, t_n) - F_\varepsilon^N U^{N, \Delta t}(x_0, t_n)\|,$$

and the rate of convergence is determined from

$$q_\varepsilon^{N, \Delta t} = \log_2 \left( \frac{r_\varepsilon^{N, \Delta t}}{r_\varepsilon^{2N, \Delta t/4}} \right).$$

The calculated maximum pointwise errors in the normalized flux  $r_\varepsilon^{N, \Delta t}$  and the corresponding order of convergence  $q_\varepsilon^{N, \Delta t}$  for Example 5.1 are given in Table 5.3 and Table 5.4. Again, one can observe the  $\varepsilon$ -uniform convergence in Table 5.3 and the first-order convergence rate in Table 5.4. In Figure 5.1 (a) and (b), the maximum pointwise errors of the solution and the normalized flux are plotted, respectively. These result reflect the first-order convergence independent of  $\varepsilon$ .

EXAMPLE 5.2. Consider the following singularly perturbed delay parabolic initial-boundary value problem:

$$(5.2) \quad \begin{aligned} u_t - \varepsilon u_{xx} + \frac{(1+x)^2}{2} u &= t^3 - u(x, t-1), & (x, t) \in (0, 1) \times (0, 2], \\ u(x, t) &= 0, & (x, t) \in [0, 1] \times [-1, 0], \\ u(0, t) &= 0, & 0 \leq t \leq 2, \\ u(1, t) &= 0, & 0 \leq t \leq 2. \end{aligned}$$



TABLE 5.1  
 Maximum pointwise error  $e_\varepsilon^{N,\Delta t}$  of the solution for Example 5.1.

$\varepsilon$	Number of intervals $N$ /Time step size $\Delta t$				
	$32/\frac{1}{10}$	$64/\frac{1}{40}$	$128/\frac{1}{160}$	$256/\frac{1}{640}$	$512/\frac{1}{2560}$
$10^0$	2.7636e-03	7.3566e-04	1.8725e-04	4.7040e-05	1.1774e-05
$10^{-2}$	6.1484e-03	1.5722e-03	3.9528e-04	9.8968e-05	2.4751e-05
$10^{-4}$	5.8657e-03	1.4826e-03	3.7294e-04	9.4594e-05	2.3439e-05
$10^{-6}$	5.5893e-03	1.4529e-03	3.6683e-04	9.2121e-05	2.3063e-05
$10^{-8}$	5.5955e-03	1.4285e-03	3.6602e-04	9.1809e-05	2.2997e-05

TABLE 5.2  
 Rate of convergence  $p_\varepsilon^{N,\Delta t}$  of the solution for Example 5.1.

$\varepsilon$	No. of intervals $N$ /Time step size $\Delta t$			
	$32/\frac{1}{10}$	$64/\frac{1}{40}$	$128/\frac{1}{160}$	$256/\frac{1}{640}$
$10^0$	1.9094	1.9741	1.9930	1.9982
$10^{-2}$	1.9674	1.9919	1.9979	1.9995
$10^{-4}$	1.9842	1.9911	1.9791	2.0129
$10^{-6}$	1.9437	1.9858	1.9935	1.9979
$10^{-8}$	1.9698	1.9645	1.9952	1.9972

As the exact solution of the problem (5.2) is not known, to obtain the accuracy of the numerical solution and also to demonstrate the  $\varepsilon$ -uniform convergence of the proposed scheme, we use the double mesh principle which is described in the following. The numerical solution is plotted in Figure 5.2 (a) and (b) for  $\varepsilon = 10^{-1}$  and  $\varepsilon = 10^{-4}$ , respectively. These figures show the existence of the boundary layers near  $x = 0$  and  $x = 1$ .

Let  $\tilde{U}^{2N,\Delta t/2}(x_i, t_n)$  be the numerical solution obtained on the fine mesh  $\tilde{D}_\varepsilon^{2N,2M} = \Omega_x^{2N} \times \Lambda_t^{2M}$  with  $2N$  mesh intervals in spatial direction and  $2M$  mesh intervals in  $t$ -direction. Then, for each  $\varepsilon$ , we calculate the maximum pointwise error by

$$E_\varepsilon^{N,\Delta t} = \max_{(x_i, t_n) \in D_\varepsilon^{N,M}} \left| U^{N,\Delta t}(x_i, t_n) - \tilde{U}^{2N,\Delta t/2}(x_i, t_n) \right|,$$

and the corresponding order of convergence by

$$P_\varepsilon^{N,\Delta t} = \log_2 \left( \frac{E_\varepsilon^{N,\Delta t}}{E_\varepsilon^{2N,\Delta t/2}} \right).$$

The calculated maximum pointwise errors  $E_\varepsilon^{N,\Delta t}$  and the corresponding order of convergence  $P_\varepsilon^{N,\Delta t}$  for Example 5.2 are given in Table 5.5 and Table 5.6, respectively. The results there show a convergence independent of the diffusion parameter  $\varepsilon$ .

The maximum pointwise errors for the solution are plotted on a log-log scale in Figure 5.3. In this figure, one can easily observe the  $\varepsilon$ -uniform convergence.

**6. Conclusions.** In this article, we solved singularly perturbed time-dependent delay reaction-diffusion problems (1.1) numerically by the upwind finite difference scheme on layer adapted nonuniform grids obtained by equidistributing the monitor function given in (3.6). A truncation error analysis and a stability analysis are provided. The proposed numerical scheme is of first-order in the temporal and second-order in the spacial variables, i.e.,  $O(\Delta t + N^{-2})$ . Error estimates for the numerical scheme are derived, which are independent of the diffusion parameter  $\varepsilon$ . Numerical results confirm the theoretical error estimate.

TABLE 5.3  
 Maximum pointwise error  $r_\varepsilon^{N,\Delta t}$  of the normalized flux for Example 5.1.

$\varepsilon$	Number of intervals $N$ /Time step size $\Delta t$				
	$32/\frac{1}{10}$	$64/\frac{1}{40}$	$128/\frac{1}{160}$	$256/\frac{1}{640}$	$512/\frac{1}{2560}$
$10^0$	2.5152e-02	1.0016e-02	4.3257e-03	2.0201e-03	9.8607e-04
$10^{-2}$	6.1271e-02	2.8039e-02	1.3411e-02	6.5732e-03	3.2593e-03
$10^{-4}$	7.5813e-02	3.2941e-02	1.5666e-02	7.7375e-03	3.4147e-03
$10^{-6}$	7.4361e-02	3.4075e-02	1.6160e-02	7.8819e-03	3.9305e-03
$10^{-8}$	7.6126e-02	3.6189e-02	1.6228e-02	7.9736e-03	3.9454e-03

TABLE 5.4  
 Rate of convergence  $q_\varepsilon^{N,\Delta t}$  of the normalized flux for Example 5.1.

$\varepsilon$	No. of intervals $N$ /Time step size $\Delta t$			
	$32/\frac{1}{10}$	$64/\frac{1}{40}$	$128/\frac{1}{160}$	$256/\frac{1}{640}$
$10^0$	1.3284	1.2113	1.0985	1.0347
$10^{-2}$	1.1278	1.0640	1.0287	1.0120
$10^{-4}$	1.2026	1.0722	1.0177	1.1801
$10^{-6}$	1.1258	1.0763	1.0358	1.0038
$10^{-8}$	1.0728	1.1571	1.0252	1.0151

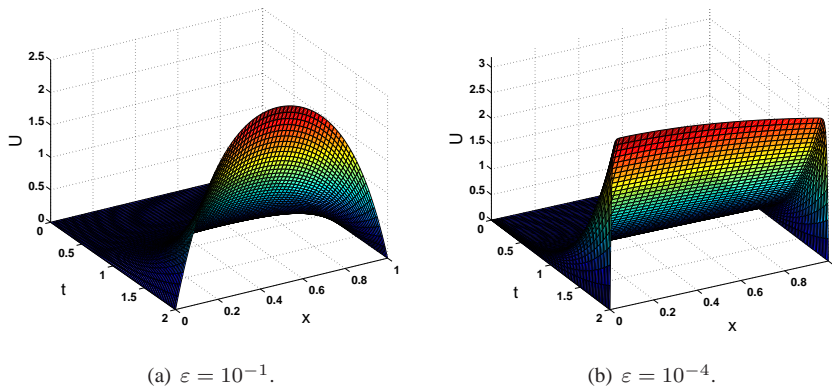


FIG. 5.2. Numerical solution of Example 5.2 for  $N = 64$  and  $\Delta t = 0.01$ .

TABLE 5.5  
 Maximum pointwise error  $E_\varepsilon^{N,\Delta t}$  of the solution for Example 5.2.

$\varepsilon$	Number of intervals $N$ /Time step size $\Delta t$			
	$32/\frac{1}{10}$	$64/\frac{1}{40}$	$128/\frac{1}{160}$	$256/\frac{1}{640}$
$10^0$	4.1424e-03	1.0515e-03	2.6387e-04	6.6030e-05
$10^{-2}$	1.5664e-01	3.9664e-02	9.9476e-03	2.4885e-03
$10^{-4}$	1.7038e-01	4.2971e-02	1.0809e-02	2.6916e-03
$10^{-6}$	1.7120e-01	4.4325e-02	1.1403e-02	2.8745e-03
$10^{-8}$	1.7083e-01	4.3954e-02	1.1329e-02	2.9009e-03

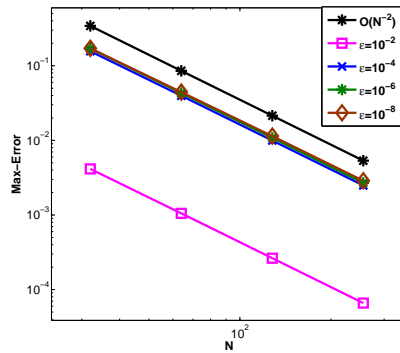


FIG. 5.3. Log-log plot for the maximum pointwise error  $E_{\epsilon}^{N, \Delta t}$  of the solution of Example 5.2.

TABLE 5.6  
 Rate of convergence  $P_{\epsilon}^{N, \Delta t}$  of the solution for Example 5.2.

$\epsilon$	No. of intervals $N$ /Time step size $\Delta t$		
	$32/\frac{1}{10}$	$64/\frac{1}{40}$	$128/\frac{1}{160}$
$10^0$	1.9780	1.9946	1.9986
$10^{-2}$	1.9816	1.9954	1.9990
$10^{-4}$	1.9874	1.9911	2.0057
$10^{-6}$	1.9495	1.9588	1.9880
$10^{-8}$	1.9585	1.9560	1.9654

**Acknowledgement.** The authors express their sincere thanks to the referee whose valuable comments helped to improve the presentation.

REFERENCES

- [1] A. R. ANSARI, S. A. BAKR, AND G. I. SHISHKIN, *A parameter-robust finite difference method for singularly perturbed delay parabolic partial differential equations*, J. Comput. Appl. Math., 205 (2007), pp. 552–566.
- [2] G. BECKETT AND J. A. MACKENZIE, *Convergence analysis of finite difference approximations on equidistributed grids to a singularly perturbed boundary value problem*, Appl. Numer. Math., 35 (2000), pp. 87–109.
- [3] ———, *On a uniformly accurate finite difference approximation of a singularly perturbed reaction-diffusion problem using grid equidistribution*, J. Comput. Appl. Math., 131 (2001), pp. 381–405.
- [4] C. CLAVERO, J. L. GRACIA, AND M. STYNES, *A simpler analysis of a hybrid numerical method for time-dependent convection-diffusion problems*, J. Comput. Appl. Math., 235 (2011), pp. 5240–5248.
- [5] P. A. FARRELL, A. F. HEGARTY, J. J. H. MILLER, E. O’RIORDAN, AND G. I. SHISHKIN, *Robust Computational Techniques for Boundary Layers*, Chapman & Hall, Boca Raton, 2000.
- [6] S. GOWRISANKAR AND S. NATESAN, *The parameter uniform numerical method for parabolic reaction-diffusion problems on equidistributed grids*, Appl. Math. Lett., 26 (2013), pp. 1053–1060.
- [7] ———, *Robust numerical scheme for singularly perturbed convection-diffusion parabolic initial-boundary value problems on equidistributed grids*, Comput. Phys. Commun., 185 (2014), pp. 2008–2019.
- [8] R. B. KELLOGG AND A. TSAN, *Analysis of some differences approximations for a singular perturbation problem without turning point*, Math. Comp., 32 (1978), pp. 1025–1039.
- [9] N. KOPEVA AND M. STYNES, *A robust adaptive method for a quasi-linear one-dimensional convection-diffusion problem*, SIAM J. Numer. Anal., 39 (2001), pp. 1446–1467.
- [10] T. LINSS, *Layer-adapted meshes and FEM for time-dependent singularly perturbed reaction-diffusion problems*, Int. J. Comput. Sci. Math., 1 (2007), pp. 259–270.

- [11] J. J. H. MILLER, E. O'RIORDAN, AND G. I. SHISHKIN, *Fitted Numerical Methods for Singular Perturbation Problems*, World Scientific, Hackensack, 1996.
- [12] J. MOHAPATRA AND S. NATESAN, *Uniform convergence analysis of finite difference scheme for singularly perturbed delay differential equation on an adaptively generated grid*, Numer. Math. Theory Methods Appl., 3 (2010), pp. 1–22.
- [13] S. NATESAN AND N. RAMANUJAM, A “booster method” for singular perturbation problems arising in chemical reactor theory by incorporation of asymptotic approximations, Appl. Math. Comput., 100 (1999), pp. 27–48.
- [14] ———, “Shooting method” for the solution of singularly perturbed two-point boundary-value problems having less severe boundary layers, Appl. Math. Comput., 133 (2000), pp. 623–641.
- [15] H.-G. ROOS, M. STYNES, AND L. TOBISKA, *Robust Numerical Methods for Singularly Perturbed Differential Equations*, 2nd ed., Springer, Berlin, 2008.
- [16] G. I. SHISHKIN, *Approximation of solutions of singularly perturbed boundary value problems with a parabolic boundary layer*, Zh. Vychisl. Mat. Fiz., 29 (1989), pp. 963–977, 1102.